# A Data-driven Approach for Fast Simulation of Robot Locomotion on Granular Media

Yifan Zhu[1], Laith Abdulmajeid[2], and Kris Hauser[1]

*Abstract*— In this paper, we propose a semi-empirical approach for simulating robot locomotion on granular media. We first develop a contact model based on the stick-slip behavior between rigid objects and granular grains, which is then learned through running extensive experiments. The contact model represents all possible contact wrenches that the granular substrate can provide as a convex volume, which our method formulates as constraints in an optimization-based contact force solver. During simulation, granular substrates are treated as rigid objects that allow penetration and the contact solver solves for wrenches that maximize frictional dissipation. We show that our method is able to simulate plausible interaction response with several granular media at interactive rates.

## I. INTRODUCTION

Physics simulators are widely used in robotics. They may be used to design and evaluate mechanisms and behaviors, and can be used inside motion planners and grasp planners to predict the outcomes of actions. Rigid body simulators model robots and objects as collections of articulated rigid bodies with either hard or spring-like point contacts with coulomb friction, and are quite commonly used [1]. Finite Element Method (FEM) simulations are used to predict the behavior of deformable materials [2], [3], and Discrete Element Method (DEM) simulations are used to predict the behavior of granular media such as sand and mud. Although FEM and DEM simulators can capture a greater variety of phenomena than rigid body simulations, their computational expense is prohibitive for most uses in robotics. For example, one study reports using 3.2 hours of computation on a 20-core processor to perform 1 s of DEM simulation for a vehicle moving on granular media composed of 150,000 bodies [4]. Hence, we ask the question, can empirical models be incorporated into rigid body simulation to efficiently simulate interaction with more complex deformable materials?

We focus on the problem of simulating robot locomotion on granular media. The interaction between a rigid foot and a granular medium is quite complex and cannot be captured accurately using analytic models. Our novel contribution is a semi-empirical simulation approach [5], [6], where a substrate contact model is first learned via extensive experiments, and then is used in a contact force solver for rigid-body simulation.

[1]: Y. Zhu and K. Hauser are with the Departments of Electrical and Computer Engineering and Mechanical Engineering and Materials Science, Duke University, Durham, NC 27708, USA. {yifan.zhu, kris.hauser}@duke.edu

[2]: L. Abdulmajeid is with the Department of Mechanical Engineering, University of Wisconsin-Madison, Madison, WI 53706, USA. laith.abdulmajeid@kaust.edu.sa

We take advantage of the stick-slip behavior of a rigid object, in our case a robot foot, moving on a granular substrate and model this interaction as a single contact resisted by a frictional wrench inside a (non-Coulomb) frictional wrench space. The wrench space varies with the foot's depth and orientation within the substrate. During data acquisition, we use a vector of parameters (referred to as the *configuration*) to define the relative pose between the foot and substrate. For a single configuration, we record a set of frictional wrenches exerted on the foot moving at different directions. The database is constructed by repeating this for a set of discrete configurations. Data can be gathered from a DEM simulation or a physical testing apparatus. DEM simulation has the advantage of easy setup and can scale using high performance computing resources, but it can be difficult to tune parameters to fit real world materials. We also constructed a physical testing apparatus in this paper.

During the simulation stage, both foot and substrate are modeled as rigid objects and are allowed to interpenetrate. The ground reaction wrench is constrained to lie within the predicted wrench space at the current foot-terrain configuration, and contact forces are calculated using a maximum dissipation principle (MDP) optimization. Due to convexity assumptions, which we find to be satisfied well in practice, the optimization problem can be solved in time polynomial in the number of robot links. As a result, we are able to simulate robot locomotion on granular media in interactive time. Simulation results are demonstrated on both a single foot and a model of the Robosimian quadruped robot traversing flat and sloped terrains composed of granular materials.

## II. RELATED WORK

Several works have studied legged motion on granular media. Some authors employ simple spring-damper [7], [8] or vistoplastic [9] models for terrain deformations. Despite the convenience of these models, they can deviate far from the empirical behavior of granular media. Xiong et al record the stress that a plate experiences when penetrating a substrate and integrates the stress to determine the stability of a robotic leg with a plate-shaped foot while standing [10]. Using this as a stability region criterion, a controller is developed to produce stable walking gaits for a planar biped traversing flat granular terrain. This model is limited to stability determination and can not predict force response while the object is moving. Li et al develop a method based on resistive force theory to predict the resistance on a thin-plate-shaped leg moving through granular media [11]. It theorizes that the net resistive force acting on an object is

the linear superposition of resistive forces on infinitesimal leg elements. They predict net force on a leg by integrating empirically-determined stress on leg elements and achieve about 30% error. This algorithm treats the penetration as a kinematic event and can not predict static stability. In contrast, our method unifies static and kinematic events and simulates dynamic motions of rigid body interacting with deformable terrains.

A related community studies off-road vehicle locomotion. Various empirical, semi-empirical and physics-based models for tire-terrain interaction have been proposed. A comprehensive survey [12] reviews the main efforts in this area. Empirical and semi-empirical methods build upon empirical tire-terrain interaction equations. Meanwhile, physics-based solutions rely on DEM and FEM simulations, which are computationally heavy [4]. Because the geometry and elastic properties of tires differ greatly from that of robot feet, the methods developed for off-road vehicles are not suitable for legged robot locomotion.

Data-driven simulation approaches have been adopted in many contexts. Bauza et al use a variation of Gaussian Process (GP) to learn the outcome of planar pushing (treated as a kinematic event) and its variability [13]. The method is able to outperform analytic models after learning only 100 pushing samples. Although it is also possible to use a pure data-driven approach in our case, we employ a semi-empirical approach to reduce the amount of training data. Another work proposes a data-driven method to predict the post-collision velocity of a planar object [14]. This method learns the optimal parameters of an analytic model given pre-impact states and outperforms pure analytic model. Our work is similar to this method in that we are also learning parameters for a contact model. However, instead of optimizing the parameters by minimizing the discrepancy between simulation and reality, we are extracting parameters directly from experiments. Wang et al use a data-driven piece-wise linear model to simulate cloth, which often has complicated nonlinear, anisotropic elastic behavior due to woven pattern and fiber properties [15]. Local stress-strain parameters are obtained by linearly interpolating the local strain and angle relative to woven pattern from a database obtained through experiments. Bickel et al use a similar approach to learn the local stress-strain relationship through Radial Basis Function (RBF) interpolation on a database of real experiment samples and use these parameters for FEM simulation [16]. Both papers are able to capture the non-linear and heterogeneous deformation behaviors of the materials studied. Like these two works, we are also learning model parameters that capture dominant physical properties and performing dynamics simulations. But in our case, rather than modeling the material stress-strain response, we are concerned with approximating the macroscopic response of granular media on a penetrating rigid object.

## III. METHODS

The structure of our method is summarized in Fig. 1. During offline learning, we run experiments on a granular
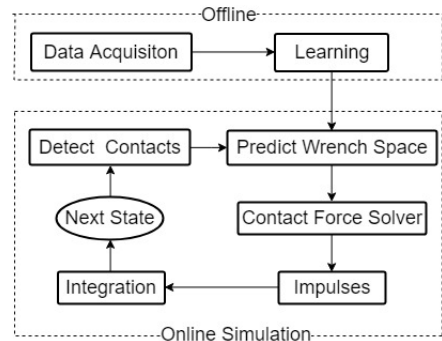


Fig. 1. The structure of our semi-empirical simulation framework.

medium to gather empirical force/torque for our contact model at different configurations. Then we learn a model to predict the wrench space for a new configurations. For each time step during online simulation, we predict the wrench space for each contact between a robot and the granular substrate. Finally, the wrench space constraints are incorporated in an optimization-based contact wrench solver.

### A. Contact Model

The interaction between rigid objects and granular media is complex, and in this work, we only model the most dominant stick-slip behavior observed in low-velocity motion. Other properties like memory effects, high-velocity inertial effects [17], force "overshoot" [10], and force fluctuations [18], are left to future work.

An object moving in granular media causes the grains around it to rearrange and slip against each other. Dry friction between the grains contributes to the majority of the resistance the object experiences. If the external force applied on an object is too weak to cause slippage between the grains, the object sits still. Studies have shown that at low speeds, velocity-independent drag force dominates [19] and this drag increases with larger penetration depth [10]. In addition, this drag is independent of the surface friction between the object and an individual grain [18].

Our proposed contact model limits the possible frictional contact wrenches between a rigid object and a substrate to a given *feasible wrench space*. In the planar case considered here we look at only a 3D wrench space (2D force and 1D torque). The reference frames in this model are shown in Fig. 2. We assume a roughly cylindrical shape of the object. Point $p_r$ is a fixed point on the object, and will be the point about which torques are measured. We define it on the central axis of the cylinder and 0.25 m away from the center of the bottom plate $p_{center}$. Point $p_c$ is the closest point on the surface of the substrate to $p_{center}$. Frame $F_c$ is centered at $p_c$ and its z-axis points is the outward normal of the surface of the substrate. Frame $F_r$ has the same orientation as $F_c$ but its origin lies on $p_r$.

The feasible wrench space $\mathcal{W}$ (Fig. 3a) is defined as a set of all wrenches $w \in \mathbb{R}^3$ that can be exerted by the substrate on the object, with forces and torques measured with respect to $F_r$. When the force and torque needed to
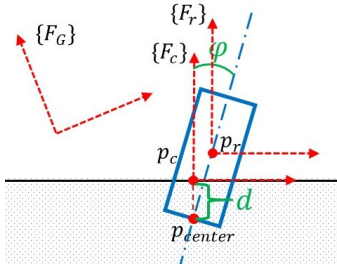
Fig. 2. Reference frames of a granular contact as described in the text. The configuration of the cylinder relative to the substrate is parametrized by $d$ and $\phi$. $F_G$ is the global frame.



(a) 3D view, with torque drawn in the out-of-plane direction.

(b) View of (a) in Fx-Fz plane.
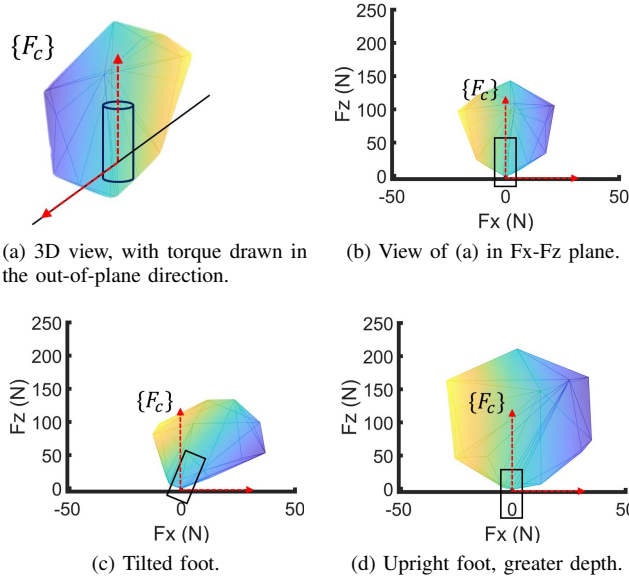
(c) Tilted foot.

(d) Upright foot, greater depth.

Fig. 3. Visualizations of the resistance wrenches faced by a rigid cylinder on pebbles.

achieve equilibrium is within $\mathcal{W}$, the object remains still. When the object starts moving/slipping, the friction resisting the object lies on the boundary $\partial\mathcal{W}$. This volume also changes depending on the depth $d$ and orientation $\phi$ of the object relative to the surface frame $F_c$. We capture dependent parameters of one object-substrate contact in a vector $\theta = (d, \phi)$. Our method uses machine learning to predict the feasible wrench space $\mathcal{W}(\theta)$, including its depth- and orientation-dependence.

It may be possible to generalize $\theta$ to include other dependent parameters, such as 3D orientation, the local geometry of the substrate, the geometry of the foot, and granular medium type. However, when more parameters are used, the amount of data needed to model $\mathcal{W}$ accurately grows rapidly. We focused on $d$ and $\phi$ to strike a balance between data acquisition difficulty and generalization.

### B. Database and Learning

*1) Data Formulation:* To model $\mathcal{W}(\theta)$ we capture points on its limit surface; this exploits the property that if $w \in \mathcal{W}$, then $cw \in \mathcal{W}$ for all $c \in [0, 1]$ [20]. Our approach moves the foot through a granular substrate in various directions and record the resistance wrenches. By the stick-slip assumption,

this populates a set of points on $\partial\mathcal{W}(\theta)$. $\mathcal{W}(\theta)$ is then approximated as the convex hull of the measured boundary wrenches. Later, we show this assumption to hold well in practice.

Specifically, we sample $n$ parameter values $\theta_1, \ldots, \theta_n$, and for each $\theta_j$ we obtain $m$ points $w_{1,j}, \ldots, w_{m,j}$ on $\partial\mathcal{W}(\theta_j)$. To obtain $w_{i,j}$, we move the foot through the substrate at the depth and orientation specified by $\theta_j$ at a given velocity $v_j$. Then, $w_{i,j}$ is simply the measured resistance wrench.

*2) Data Acquisition:* It may be tempting to gather these measurements simply by moving to a given value of $\theta$, and executing short movements with different velocities. However, this poorly ensures that the medium is in slip phase, due to elastic deformation and force overshoot [10]. Moreover, the medium is disturbed and compacted when the foot moves through it, which runs the risk of inconsistent measurement due to irregular loading. To address these issues, our acquisition method executes longer controlled trajectories and resets the material in-between runs.

For one run with parameter $\theta_{des}$ and velocity $v_{des}$, both defined with respect to $F_c$, we prepare the substrate in a consistent manner and follow a constant-velocity trajectory that passes through $\theta_{des}$. We record the resistance along the trajectory, filter it, and then obtain a wrench estimate at the instant when the foot is at $\theta_{des}$.

Specifically, we choose the duration of the whole trajectory to be $t_{total}$ and pass $\theta_{des}$ at $0.8 \cdot t_{total}$, which is chosen for consistency of repeated measurements. The process follows these steps, as shown in Fig. 5:

1) Prepare the surface such that it is flat and not compacted.
2) Move the foot from above the granular surface directly to the starting point of the trajectory. This point is $\theta_{des} - 0.8t_{total}v_{des}$.
3) Start moving at velocity $v_{des}$ for duration $t_{total}$, while recording force, torque and position.
4) Filter the data with a low-pass filter to remove noise. Calculate exactly when the configuration reaches $\theta_{des}$ and record the wrench at this time.
5) Transform the wrench to frame $F_r$.

The simulation and real robot setup we use for acquiring data is shown in Fig. 4. Simulation is performed using YADE [21], an open-source DEM software, where a floating cylinder is moved through a box of 58,500 spheres. The robot we use is Robosimian, a quadruped with 28 active degrees of freedom and F/T sensors on the ends of its four limbs. One of the feet is driven through a container filled with a granular medium and acquire measurements with the F/T sensor connecting the foot and ankle links.

*3) Learning:* Our database consists of $n$ parameter values $\theta_1, \ldots, \theta_n$, and for each $\theta_j$ we have $m$ extreme wrenches $w_{1,j}, \ldots, w_{m,j}$ on $\partial\mathcal{W}(\theta_j)$. To model $\partial\mathcal{W}(\theta)$, we learn $m$ regression models that predict the $m$ extreme wrenches for a novel value of $\theta$. Specifically, each wrench regression $w_i(\theta)$ is learned so that $w_i(\theta_j) \approx w_{i,j}$ for $j = 1, \ldots, n$.

Experiments find that Radial Basis Function (RBF) interpolation, Gaussian Process (GP), and SVM regression
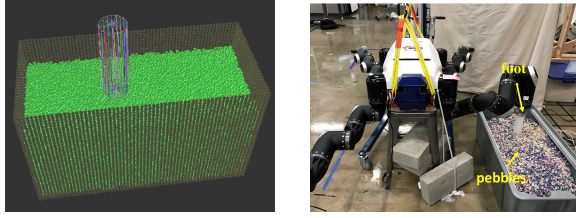
(a) Simulation setup in the DEM simulator YADE for data acquisition. (b) Data acquisition apparatus with Robosimian.

Fig. 4. Data acquisition is performed in simulation or a physical robot.
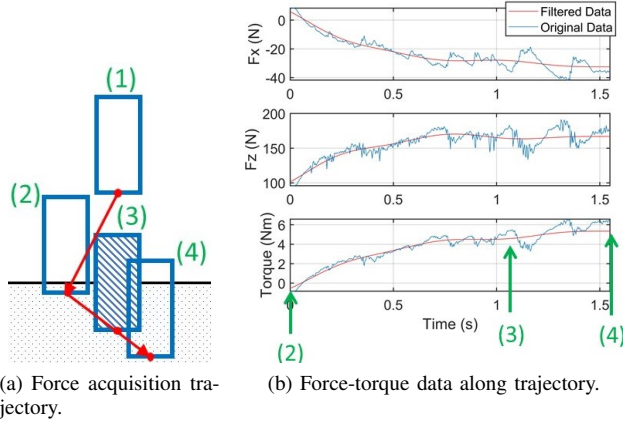


(a) Force acquisition trajectory. (b) Force-torque data along trajectory.

Fig. 5. The robot foot trajectory for a run with $\theta_{des} = [-0.03, \frac{\pi}{2}, 0]$ and $v_{des} = [0.014, -0.014, 0]$ in sand. The four milestones are: (1) starting pose for the foot, (2) start of the constant velocity trajectory, (3) the robot reaches $\theta_{des}$, (4) end of trajectory.

achieve similar performance. Results using 5-fold cross validation show that RBF interpolation outperforms GP and SVM slightly on our dataset, so we use it in our experiments.

In order to approximate $\mathcal{W}(\theta)$, we then take the convex hull of $w_1(\theta), \ldots, w_m(\theta)$ and represent the feasible set using the minimal half-space represention:

$$A(\theta)w \leq b(\theta). \tag{1}$$

### C. Simulation Framework

Our simulation framework is built upon the work of [22], which solves for contact forces based on the Maximum Dissipation Principle (MDP). Specifically, at each time step the simulation calculates the friction forces maximize the rate of energy dissipation, i.e., minimizing kinetic energy at the next simulation frame. Compared to more traditional linear complementary problem (LCP) methods [23], [24], this method has comparable accuracy and is more convenient for extending simulations beyond Coulomb friction models.

When applying MDP to our case, we note that the movement of particles in the granular substrate also contributes KE to the system. While we cannot know the microscopic movements of all the particles, we assume that the aggregate velocity of the particles is a multiple of the velocity at the bottom of the foot. Our approach then minimizes the sum of the KE of simulated bodies and the approximated KE of granular particles.

We use generalized coordinate representation, and define the following notation:

- $h$: time step size
- $q$, $v$: generalized coordinates and velocities
- $u$: joint torque control inputs
- $k$: generalized external forces
- $M$: generalized inertia matrix
- $J_u$: joint control torque jacobian
- $c_t$: stacked vector of contact wrench impulses
- $c_j$: stacked vector of joint constraint impulses
- $J_t$: contact wrench Jacobian
- $J_c$: joint constraint Jacobian
- $J_p$: $p_{center}$ velocity Jacobian
- $M_g$: mass matrix of the granular particles

During each simulation step, a contact detector examines whether foot $i$ penetrates the granular medium, and if so, calculates the contact parameters $\theta_i$. We clamp $\phi_i$ to be between $-\frac{\pi}{2}$ and $\frac{\pi}{2}$ because more extreme angles would be quite far from the sampled data. The bodies are considered to be in contact when $d_i$ is negative. The foot may still touch the substrate if $d_i > 0$ and $\phi_i \neq 0$. However, since the resistance is small in this case, we ignore it for simplicity. For wider feet, one might not want to leave this out. For each contact, we predict its corresponding feasible wrench space $\mathcal{W}(\theta_i)$ using the learned model in the foot's local reference frame, rotate it to the global frame if it is on a slope and convert it to half-space representation.

Then, we calculate the joint and contact wrench impulses by solving the following optimization problem:

$$\min_{c_t, c_j} \quad v^{t+1^T} M v^{t+1} + (J_p v^{t+1})^T M_g (J_p v^{t+1}) \text{ s.t.}$$

$$J_c v^{t+1} = 0$$

$$h A_1(\theta_1) c_{t_1} \leq b_1(\theta_1) \tag{2}$$

$$\vdots$$

$$h A_N(\theta_N) c_{t_N} \leq b_N(\theta_N).$$

In this problem, the velocity on the next time step is $v^{t+1} = M^{-1}(J_t^T c_t + J_c^T c_j + J_u^T u + h k) + v^t$. The second term in the objective represents the kinetic energy of the granular substrate. $J_p$ transforms the velocity at center of mass of each foot to that at $p_{center}$. $M_g$ is used to approximate the aggregate momentum of change of the grains as a function of the velocity of $p_{center}$. The resulting problem is a QP and can be solved in polynomial time. The position is then updated according to $q^{t+1} = q^t + h v^{t+1}$.

## IV. EXPERIMENTS AND RESULTS

### A. Data Generation

We test on 1 granular medium in DEM simulation and 2 physical media. The DEM simulation medium (Beads) uses particles with the following properties:

- Young's modulus: $3 * 10^8$
- Poisson's ratio: $0.3$
- Density: $1631 \, \text{kg/m}^3$
- Coefficient of friction: $0.577$

Fig. 6. Pebbles and sand used in our experiments. A 0.25 USD coin is shown for scale.

| Medium | Depth $d(m)$ | Tilt $\phi(rad)$ |
|---|---|---|
| Beads | [0,-0.06,-0.12,-0.18,-0.24] | [0,0.25,0.5,0.75,1,1.25,1.5] |
| Pebbles | [0,-0.015,-0.03,-0.045] | [0,0.3,0.6,0.9] |
| Sand | [0,-0.01,-0.03,-0.05,-0.07] | [0,0.3,0.6,0.9] |

- Shape: spheres with radius of 0.01 m.

The physical granular media are pond pebbles with diameter of about 0.8-1.0 cm (Pebbles) and fine play sand (Sand), shown in Fig. 6.

We sample $n$ configurations on a grid of $d$ and $\phi$. The ranges respect the size of the foot and the torque limits of the robot, such that the foot does not get submerged completely into the medium or exceed the stall force of the robot. The resolution of the grid is chosen according to practical time and computational resource limitations. Table I summarizes the the grid parameters. At zero depth, we do not run any experiments and set all wrenches to zero. Also, to achieve better data efficiency, we exploit symmetry in the foot shape, so that the wrench space of $(d_i, \phi_i)$ has the same shape as that of $(d_i, -\phi_i)$, but with the signs of force in the x direction and torque flipped.

For each configuration, we sample a uniform grid of $m$ velocities on the surface on a 3D unit sphere using spherical coordinates. The unit velocities are then scaled in the x, z, and $\phi$ axes by (0.2m/s, 0.2m/s 0.6 rad/s) for Beads and (0.02m/s, 0.02m/s 0.3 rad/s) for Pebbles and Sand. The discrepancy comes from the fact that the latter two are much stiffer and the robot foot cannot penetrate into them too much. For DEM simulation, we collect data for m=26 and m=58. Running our simulators using these two different densities of sampling, we do not observe a significant difference in the object's post-contact motion. For real world experiments, which are more time consuming, we collect data for m=26 only.

### B. Validity of Convexity Assumption

We evaluate the extent to which the wrench space convexity assumption holds. As a concavity metric, we use the relative distance between the convex hull surface and innermost point in the convex hull. Specifically, for a given $\theta_j$ this dimensionless measure is Concavity$_j = \max_i((b(\theta_j) - A(\theta_j)w_{i,j})/\|w_{i,j}\|)$. To avoid points with small magnitude, we exclude data where depth is zero, or the magnitude of the point is less then 1. If all of the inner points are less than 1,

| Medium | Average Concavity | Worst Concavity |
|---|---|---|
| Beads | 0.0174 | 0.1207 |
| Pebbles | 0.0013 | 0.0155 |
| Sand | 0 | 0 |



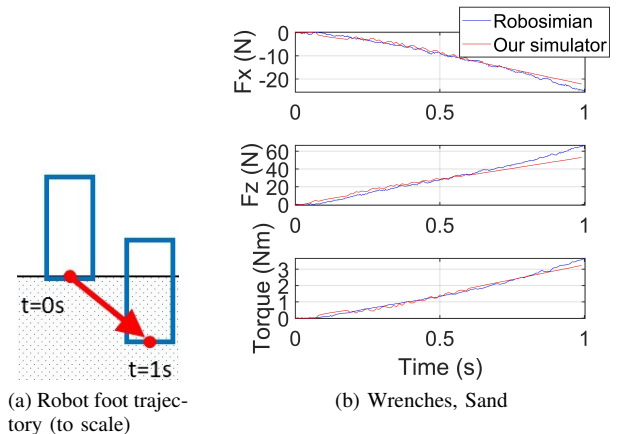(a) Robot foot trajectory (to scale)

(b) Wrenches, Sand

Fig. 7. Comparing measured wrenches between the physical Robosimian and our simulator using a straight path and the Sand medium.

we treat the concavity as zero. Tab. II lists for each medium the average concavity across configurations as well as the worst case. Most of the wrench spaces are convex. There are only a few wrench spaces with concavity larger than 10%, and these occur at wrenches with small magnitudes.

### C. Simulation Experiments

*1) Accuracy Test:* To evaluate the accuracy of our method, we command a foot to follow a trajectory and compare the resistance on the robot acquired from experiments and our simulator. Our simulator uses a simple PID controller to follow the reference trajectory. The mass and the moment of inertia of the simulated foot are $7.357\,\mathrm{kg}$ and $0.061\,\mathrm{kg \cdot m^2}$. The PID gains being used are $K_p = [8000, 20000, 300]$, $K_i = [4000, 6000, 1000]$ and $K_d = [200, 400, 10]$. $M_g$ is tuned empirically by matching simulated and measured trajectories and wrenches, and we use $M_g = diag(14.714, 14.714, 0.122)$, which is twice the inertia of the foot.

Fig. 7 shows a good match between the simulated resistance and measured resistance on a straight trajectory in Sand, showing resistance force and torque increasing with depth. This is similar for Pebbles medium and is not shown here. Results for a curved path in Pebbles are shown in Fig. 8b. The simulator is able to predict the general trend and approximate magnitudes of the resistance. However, the simulated resistance stays high as the downward movement slows, while the actual resistance drops. We believe that the discrepancy is caused by un-modelled memory effects, such as compaction, and some integral wind-up from the simulated PID controller. Modeling memory effects would be an interesting problem for future work.
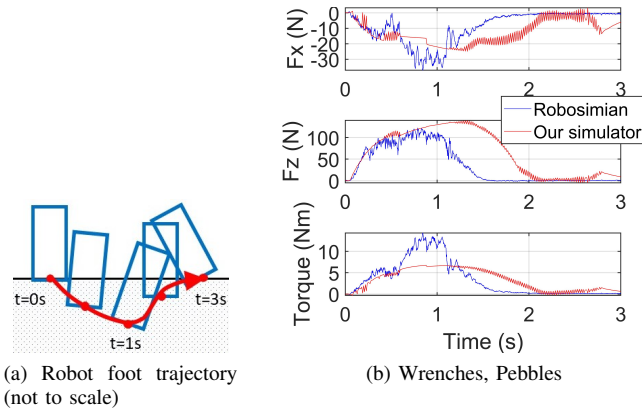
(a) Robot foot trajectory (not to scale)

(b) Wrenches, Pebbles

Fig. 8. Comparing measured wrenches between physical Robosimian and our simulator using a curved path and the Pebbles medium.



(a) Drop on a slope.

(b) Tilted drop on a flat surface.

Fig. 9. Drop tests.



(a) Pushing the front feet forward. Because the rear legs are sunk deeper in the sand, they resist motion more, so the front feet slip.



(b) A trot gait showing deeper penetration during the two-foot phase.



(c) Sliding on a slope and eventually stopping, with joints fixed. The red and green lines show the trace of the front and rear feet, respectively. The snapshots of the robot are from the simulation on pebbles.

Fig. 10. Locomotion tests with different terrains on a simplified 2D Robosimian model facing right.
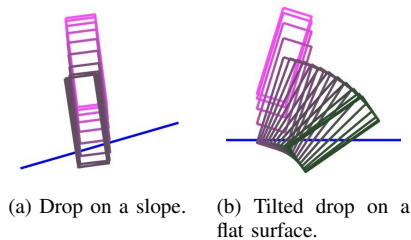
*2) Drop Test with a Single Foot:* Next, we perform a test of dropping behavior with one single object. We drop the object from a small height at two different surface orientations, displayed in Fig. 9. When the object is dropped in vertical orientation of flat terrain, it remains erect. In slightly sloped terrain, the object begins to tip, but ultimately is able to balance because the medium is able to provide a resistance torque. When slightly tilted at 0.2 radian, the object tips over and eventually stops on a flat surface.

*3) 2D Quadruped Locomotion Test:* Our next tests perform a highly simplified model of the sagittal movement of a quadruped walking on soft terrain. Fig. 10 shows images from the resulting animations. Note that the robot faces to the right of the pageand the simulated terrain is sand, if not specified. In the first simulation, the robot has its weight shifted to the rear legs and pushes the front feet forward. Because the rear feet are able to resist a larger force, only the front feet slip. The second simulation is one trotting gait, where the diagonal two limbs move simultaneously. The feet sink and lift realistically as the weight of the body shifts. In the third simulation, the robot is dropped onto a sloped terrain, with its joints locked. The robot initially slides and accelerates, but eventually stops when the terrain flattens. Pebbles allow shallower penetration and stops the robot at a higher potential energy, compared to sand. This is expected because pebbles are able to provide greater resistance force at the same penetration depth.

*4) Computation Speed:* In this test, we use a more complicated quadruped model that includes 1 body and 4 limbs, with each limb consisting of 2 links and 1 foot. In total, a 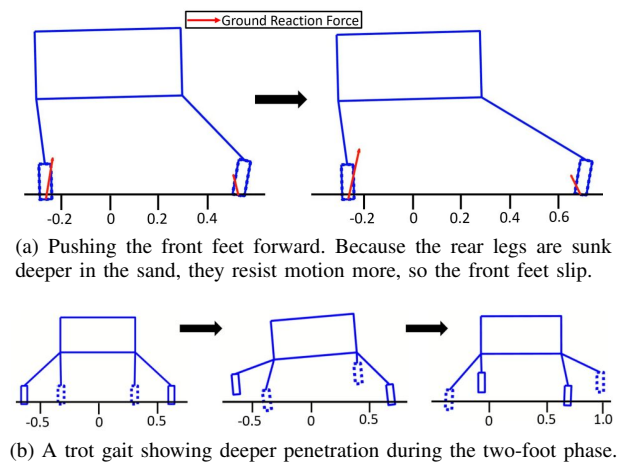system of 13 rigid bodies and 12 revolute joints are simulated in Matlab on a standard PC with an Intel i7 2.4GHz processor. The resultant optimization problem has 4 contacts, 36 variables, 24 constraints associated with joints, and 4 sets of constraints from granular contacts. One frame on average takes about 0.343 s to compute, with about 90% of the time spent on solving the optimization, and about 5% on interpolating the wrench spaces. By utilizing a complied language and a more task-specific convex optimization package, we expect to speed up computation significantly.

## V. CONCLUSION

This paper proposed a contact model for rigid objects and granular media to capture depth-dependent stick-slip phenomena. We present a procedure to acquire data-driven feasible wrench spaces and learn the parameters for this contact model. An optimization-based rigid contact force solver is developed to use this data to simulate continuous granular contact with multiple contacts at interactive rates. Future work should consider improving the prediction accuracy by incorporating memory effects of granular material like compaction and pile formation. Also, it is important to examine improving the data efficiency of the learning approach as more parameters are included in the model, which makes generalization more challenging.

## REFERENCES

[1] T. Erez, Y. Tassa, and E. Todorov, "Simulation tools for model-based robotics: Comparison of Bullet, Havok, MuJoCo, ODE and PhysX," *IEEE Int. Conf. Rob. Aut.*, vol. 2015-June, no. June, pp. 4397–4404, 2015.

[2] Y. Bai and C. K. Liu, "Coupling cloth and rigid bodies for dexterous manipulation," in *MIG*, New York, New York, USA, 2014, pp. 139–145.

[3] D. M. Conachie, M. Ruan, and D. Berenson, "Interleaving Planning and Control for Deformable Object Manipulation," *Int. Sym. on Robotics Research*, pp. 1–16, 2017.

[4] A. Tasora, R. Serban, H. Mazhar, A. Pazouki, D. Melanz, J. Fleischmann, M. Taylor, H. Sugiyama, and D. N. B, "Chrono: An open source multi-physics dynamics engine," in *International Conference on High Performance Computing in Science and Engineering*, 2015, pp. 19–49.

[5] R. J. Wilman, L. Miller, M. J. Jarvis, T. Mauch, F. Levrier, F. B. Abdalla, S. Rawlings, H.-R. Klckner, D. Obreschkow, D. Olteanu, and S. Young, "A semi-empirical simulation of the extragalactic radio continuum sky for next generation radio telescopes," *Monthly Notices of the Royal Astronomical Society*, vol. 388, no. 3, jun 2008.

[6] M. I. Mendelev, M. J. Kramer, C. A. Becker, and M. Asta, "Analysis of semi-empirical interatomic potentials appropriate for simulation of crystalline and liquid Al and Cu," *Philosophical Magazine*, vol. 88, no. 12, pp. 1723–1750, 2008.

[7] H.-j. Kang, K. Hashimoto, K. Nishikawa, E. Falotico, H.-o. Lim, A. Takanishi, C. Laschi, P. Dario, and A. Berthoz, "Biped walking stabilization on soft ground based on gait analysis," *IEEE Int. Conf. Biomed. Rob. and Biomech.*, no. 2, pp. 669–674, 2012.

[8] C. M. Hubicki and J. W. Hurst, "Running on Soft Ground: Simple, Energy-Optimal Disturbance Rejection," *Int. Conf. Climb. Walk. Rob. Supp. Tech. Mobi. Mach.*, pp. 543–547, 2012.

[9] V. Vasilopoulos, I. S. Paraskevas, and E. G. Papadopoulos, "Compliant terrain legged locomotion using a viscoplastic approach," *IEEE/RSJ Int. Conf. Intel. Rob. Sys.*, no. Iros, pp. 4849–4854, 2014.

[10] X. Xiong, A. D. Ames, and D. I. Goldman, "A stability region criterion for flat-footed bipedal walking on deformable granular terrain," in *IEEE/RSJ Int. Conf. Intel. Rob. Sys.* IEEE, sep 2017, pp. 4552–4559.

[11] C. Li, T. Zhang, and D. I. Goldman, "A Terradynamics of Legged Locomotion on Granular Media," *Science*, vol. 339, no. 6126, pp. 1408–1412, mar 2013.

[12] S. Taheri, C. Sandu, S. Taheri, E. Pinto, and D. Gorsich, "A technical survey on Terramechanics models for tire-terrain interaction used in modeling and simulation of wheeled vehicles," *Journal of Terramechanics*, vol. 57, pp. 1–22, 2015.

[13] M. Bauza and A. Rodriguez, "A probabilistic data-driven model for planar pushing," *IEEE Int. Conf. Rob. Aut.*, pp. pp. 3008–3015, apr 2017.

[14] N. Fazeli, S. Zapolsky, E. Drumwright, and A. Rodriguez, "Learning Data-Efficient Rigid-Body Contact Models: Case Study of Planar Impact," *Conf. on Robot Learning*, 2017.

[15] H. Wang, J. F. O'Brien, and R. Ramamoorthi, "Data-Driven Elastic Models for Cloth: Modeling and Measurement," *ACM Transactions on Graphics*, vol. 30, no. 4, p. 1, 2011.

[16] B. Bickel, M. Bächer, M. A. Otaduy, W. Matusik, H. Pfister, and M. Gross, "Capture and modeling of non-linear heterogeneous soft tissue," in *ACM SIGGRAPH 2009 papers on - SIGGRAPH '09*, New York, New York, USA, 2009, p. 1.

[17] T. A. Brzinski, P. Mayor, and D. J. Durian, "Depth-Dependent Resistance of Granular Media to Vertical Penetration," *Physical Review Letters*, vol. 111, no. 16, p. 168002, oct 2013.

[18] I. Albert, P. Tegzes, B. Kahng, R. Albert, J. G. Sample, M. Pfeifer, A. L. Barabási, T. Vicsek, and P. Schiffer, "Jamming and fluctuations in granular drag," *Physical Review Letters*, vol. 84, no. 22, pp. 5122–5125, 2000.

[19] R. Albert, M. A. Pfeifer, A. L. Barabási, and P. Schiffer, "Slow drag in a granular medium," *Physical Review Letters*, vol. 82, no. 1, pp. 205–208, jan 1999.

[20] K. Hauser, S. Wang, and M. R. Cutkosky, "Efficient Equilibrium Testing Under Adhesion and Anisotropy Using Empirical Contact Force Models," *IEEE Transactions on Robotics*, vol. PP, pp. 1–13, 2018.

[21] J. Kozicki and F. Donze, "YADE-OPEN DEM: an open-source software using a discrete element method to simulate granular material," *Engineering Computations*, vol. 26, no. 7, pp. 786–805, 2009.

[22] E. Drumwright and D. A. Shell, "Modeling contact friction and joint friction in dynamic robotic simulation using the principle of maximum dissipation," *Springer Tracts in Advanced Robotics*, vol. 68, no. STAR, pp. 249–266, 2010.

[23] D. Baraff, "Fast contact force computation for nonpenetrating rigid bodies," *SIGGRAPH*, pp. 23–34, 1994.

[24] M. Anitescu and F. Potra, "Formulating Multi-Rigid-Body Contact Problems with Frictionas Solvable Linear Complementarity Problems," *ASME Journal of Nonlinear Dynamics*, vol. 14, no. 93, pp. 231–247, 1997.